Sustainable Chemistry and Pharmacy 42 (2024) 101761

Contents lists available at ScienceDirect

Sustainable Chemistry and Pharmacy

journal homepage: www.elsevier.com/locate/scp

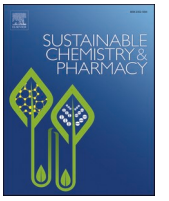

# Exploring the potential of a waste-derived bone char for pharmaceuticals adsorption in saline-based wastewater

Catarina Miranda [a], Francesca Scalera [b], Andreana Piancastelli [c], Robert C. Pullar [d], Maria Elizabeth Tiritan [e,f], Clara Piccirillo [b,*], Paula M.L. Castro [a], Catarina L. Amorim [a]

[a] Universidade Católica Portuguesa, CBQF – Centro de Biotecnologia e Química Fina – Laboratório Associado, Escola Superior de Biotecnologia, 4169-005 Porto, Portugal
[b] CNR NANOTEC, Institute of Nanotechnology, Campus Ecoteckne, Lecce, 73100, Italy
[c] Institute of Science, Technology and Sustainability for Ceramics (ISSMC), National Research Council (CNR), Faenza (RA), Italy
[d] Department of Molecular Sciences and Nanosystems (DSMN), Ca' Foscari University of Venice, 30172 Venezia Mestre, Italy
[e] Laboratório de Química Orgânica e Farmacêutica, Departamento de Ciências Químicas, Faculdade de Farmácia do Porto, Portugal
[f] Centro Interdisciplinar de Investigação Marinha e Ambiental (CIIMAR), Universidade do Porto, Portugal

ARTICLE INFO

Handling Editor: Borhane Mahjoub

*Keywords:*
Tuna bone char
Pharmaceuticals
Tramadol
Venlafaxine
Adsorption
Remediation

ABSTRACT

In this study, the effect of salinity in wastewater on the adsorption capacity of a bone char material prepared through pyrolysis of tuna bones at 1000 °C was investigated for two pharmaceuticals, tramadol (TRA) and venlafaxine (VNF), both contaminants of emerging concern. This is the first time that the adsorption efficiency of a bone char-type material was tested in such conditions.

The Tuna Bone Char (TBC) was composed of calcium phosphate (hydroxyapatite), and graphitic carbon. The TBC is a nanostructured material (particle size 30–60 nm), with a surface area of 100.67 $m^2/g$ (higher than other waste-derived type materials), and a total pore volume of 575.2 $mm^3/g$.

TBC capacity to adsorb TRA and VNF, individually or combined, was evaluated in batch experiments using different aqueous matrices: water, non-saline wastewater, and wastewaters with different salinity levels (7.5 and 12 g/L).

For individual pharmaceuticals, the TBC had a higher affinity for TRA than VNF. The presence of salts in wastewaters led to a decrease in the TBC adsorption capacity but it was still effective for pharmaceuticals adsorption. Indeed, for the individual pharmaceuticals, the TBC adsorption capacity ($q_t$) was 0.72–2.14 and 0.77–1.70 mg/g for TRA and VNF respectively, depending on the aqueous matrix. With both pharmaceuticals present, lower $q_t$ values were experimentally obtained for TRA and VNF.

The potential of the TBC, a material derived from a by-product of the fish industry, to be used for environmental remediation in different environments, such as saline wastewaters was demonstrated, widening the range of its potential applications.

* Corresponding author.
*E-mail address:* clara.piccirillo@nanotec.cnr.it (C. Piccirillo).

https://doi.org/10.1016/j.scp.2024.101761
Received 24 May 2024; Received in revised form 5 August 2024; Accepted 28 August 2024

## 1. Introduction

Water scarcity and pollution pose significant global challenges, threatening the availability of clean and safe water for the whole world population. Attending these issues is fundamental to fulfilling the Sustainable Development Goals from the United Nations, particularly goal 6, which aims to ensure the availability of water and sanitation for all. Only by facilitating access to clean water, with reduced levels of micropollutants, is possible to protect and preserve the ecosystems and their biodiversity aligned with goal 14, as well as to ensure health and well-being across all age groups, as outlined in goal 3.

Access to clean water has always been a challenge for our society and achieving this objective is becoming even more difficult. On one side, the rise in population density implies a huge water demand, at the same time, intensive human activities (i.e. industry or agriculture) may lead to a rise in the water pollution levels. In addition, in recent years, the growing occurrence of contaminants of emerging concern (CECs) in aqueous environmental matrices has been attracting increased awareness. CECs consist of a broad range of pollutants which include pharmaceuticals and hormones, pesticides, personal care products, illicit drugs and perfluorinated compounds, among others. CECs have been detected in wastewaters at concentrations ranging from ng/L to mg/L (Golovko et al., 2021). The detection concentration range for pharmaceuticals is typically lower, varying from ng/L to μg/L (Hernández-Tenorio et al., 2022), but some pharmaceuticals have been detected in pharmaceutical industry wastewaters at concentrations up to mg/L (Bielen et al., 2017). CECs are poorly removed in wastewater treatment processes, which results in their accumulation in various environmental matrices, potentially causing adverse effects on ecosystems and human health (Bangia et al., 2023). Indeed, the occurrence, risks and sources of CECs in water bodies have been topics of interest. In the case of pharmaceuticals, their increased production, prescription, and consumption led to their frequent detection in wastewater treatment streams and watercourses that receive their discharges (Egli et al., 2023; James et al., 2023; Montes et al., 2023). The antidepressant venlafaxine (VNF), which belongs to the selective serotonin and norepinephrine reuptake inhibitors class, has been extensively consumed worldwide because of the increasing number of clinical cases of anxiety and depression, inevitably ending up in watercourses (Kodešová et al., 2024). Indeed, some of its harmful effects on aquatic life have been reported (Ribeiro et al., 2022; Sehonova et al., 2019). Recently this pharmaceutical was included in the 3rd Watch List from the European Union (Gomez Cortes et al., 2020). Another widely prescribed pharmaceutical is Tramadol (TRA), an analgesic drug, used as a painkiller to treat acute and chronic pain and which also functions as an off-label anxiolytic and antidepressant. This drug has been detected in wastewater treatment effluents and surface waters, which ultimately can affect several tissues of fish living in contaminated ponds and streams (Ghazouani et al., 2022; Grabicová et al., 2020; Silva et al., 2017). Moreover, VNF and TRA are both chiral pharmaceuticals. Though chiral compounds have similar chemical structures, they exhibit distinct three-dimensional spatial configurations and their structures are non-superimposable mirror images of each other (Ribeiro et al., 2012). As these chiral compounds may occur in environmental matrices as individual enantiomers or as mixtures of the two enantiomers, it is important to monitor the behavior of both enantiomers in remediation strategies (Barreiro et al., 2021).

Apart from CECs, wastewater treatment plants (WWTPs) are often challenged by the variable salinity levels in the wastewater. The presence of salts in wastewater can arise from diverse sources, namely sanitary (e.g., toilet flushing), industrial processes (e.g., washing and defrosting procedures) or high-pressure procedures (e.g., desalination plants), amongst others (Ching and Redzwan, 2017; Li et al., 2018; Panagopoulos, 2020). More recently, the seawater intrusion phenomenon in WWTPs has been intensifying, thus altering the salinity levels of the wastewater, which fluctuate from low to high levels over the day. The chemical complexity of the wastewater with the co-occurrence of stressors like salts and CECs often represents an obstacle for the removal effectiveness of WWTPs as these stressors can interfere with the biological treatment processes. Adsorption-based processes have emerged as promising systems to mitigate the release of more recalcitrant contaminants, such as pharmaceuticals, in receiving watercourses. However, complex matrices such as wastewater can present unique challenges to the adsorption process due to their heterogeneous chemical composition, containing various dissolved compounds, including salts and CECs, which may directly influence the adsorption process. Literature reports contrasting results on the effect of different salinity levels in adsorption-based processes. Some studies showed no significant variations in the materials' removal efficiency (Hajji Nabih et al., 2023; Tsai et al., 2022), while in other cases, either an increase (Goh et al., 2022; Lamichhane et al., 2016) or a decrease (Singh et al., 2022) were observed. Considering that CECs are a very wide class of molecules, with different functional groups and chemical characteristics, they can interact differently with the adsorption materials. Likewise, each sorbent material has its properties which can also affect the adsorption process. Therefore, it is of major importance to consider the complex interactions between adsorbents and contaminants, when assessing the potential of an adsorption material. Lately, among the several adsorption materials available for use, particular interest has been given to those derived from by-products of industrial processes, in particular the ones from the agro-food sector, as a way to promote the circular economy concept. Residues containing mainly carbon in their composition have been used to prepare graphitic-based adsorption materials through pyrolysis, usually known as biochars (Hajji Nabih et al., 2023). During the pyrolysis process, the organic matter is converted into inorganic graphitic carbon (Hu and Gholizadeh, 2019). Due to the gas released during the pyrolysis, the resulting powders often have a high surface area turning them into effective adsorption materials. Bones are a waste by-product of both fish and meat industries that could be used to prepare carbon-based materials, thus reusing a waste. Through the pyrolysis of these waste by-products, it is possible to obtain a material known as bone char (BC). BC has been recognized as one of the adsorbents with the least adverse impact on human and environmental health, especially in comparison with other types of adsorbents, such as aluminum oxide and wood charcoal, among others (Medellín-Castillo et al., 2023). Like biochar, BC possesses a high surface area, when prepared by pyrolysis. However, differently from biochar, BC contains inorganic calcium phosphate, generally in the form of hydroxyapatite ($Ca_{10}(PO_4)_6(OH)_2$) (Alkurdi et al., 2020), and the presence of this group in BC chemical composition confers excellent adsorption potential for several types of contaminants. Moreover, the multiphasic composition of BC containing both graphitic carbon and calcium phosphate groups enlarges this material's adsorption capacity as additional binding sites for contaminants adsorption are available (Piccirillo, 2023).

Literature reports the enhanced effectiveness of BC-type materials for the removal of several pollutants, such as phenol (Lima et al., 2024), nitrobenzene (Ahmad et al., 2023), crystal violet (Cruz et al., 2020), methylene blue (Ghanizadeh and Asgari, 2011), sodium dodecyl sulfate (Hashemi et al., 2013), fluoride (Brunson and Sabatini, 2014), boron (Valverde et al., 2023) or heavy metals (Park et al., 2015). BC adsorption capacity was tested on pharmaceuticals such as diclofenac and fluoxetine (Piccirillo et al., 2017) and naproxen (Reynel-Avila et al., 2015), but this field needs more investigation, especially regarding the adsorption process in aqueous matrices with complex chemical composition.

The present work aims to explore the capacity of tuna bone char (TBC), a powder BC-type material obtained through the pyrolysis of tuna bone wastes provided by a fish processing industry, to adsorb two distinct pharmaceuticals from aqueous matrices with different compositions, some mimicking real urban wastewater with different levels of salinity. The chiral pharmaceuticals VNF and TRA were selected as model compounds for this study. The objective of the study is to understand if the matrix chemical composition and its salt ions levels affect the efficiency of the TBC material for adsorbing pharmaceuticals supplied individually or in a mixture. To the best of our knowledge, this is the first time that this kind of investigation was performed and possible interferences due to the presence of salts in the matrix composition were considered. This study goes beyond the state of the art as it could widen the application of BC-like materials to wastewaters with different salinity levels.

## 2. Materials and methods

### 2.1. Chemical reagents

99% Tramadol hydrochloride and 98% Venlafaxine hydrochloride were purchased from Merck (Germany) and TCI (Japan), respectively. 99.9% Ethanol gradient grade for liquid chromatography from Merck and 98% Ammonium acetate from PanReac Applichem (Italy) were used for the preparation of the mobile phase. 99% Glacial acetic acid from Carlo Erba Reagents (Italy) was used for pH adjustment of the mobile phase.

### 2.2. TBC preparation and characterization

Tuna bones were kindly supplied by Mare Aperto Food SRL (Genova, Italy). The bones were cleaned from residual meat with hot water. To prepare the TBC, a pyrolysis process was performed using a Nabertherm RHTH 120–600/16 high-temperature tube furnace (horizontal design). Before the pyrolysis, high vacuum conditions were achieved with a turbomolecular pump (Turbolab 80); successively ambient pressure was reached with a flow of oxygen-free dry nitrogen, whose flow was maintained during the whole pyrolysis process. The pyrolysis was performed up to 1000 °C, with a heating ramp of 5 °C/min and a dwell time of 1 h. Previous studies showed that applying such high pyrolysis temperature would allow for a more complete graphitic carbon formation (Tomczyk et al., 2020) as well as a higher release of gases that will lead to materials with higher surface area (Côrtes et al., 2019). Also, a previous study has shown that fish-bone char exhibited better adsorption performance for pharmaceuticals when pyrolyzed at higher temperatures (1000 °C) (Piccirillo et al., 2017).

The pyrolyzed bones were manually milled into powder and mechanically milled with an automatic grinder (CH-MT120), at a speed of 90 rpm for 3 h.

The TBC powder was analyzed with Fourier-transform infrared spectroscopy (FTIR) to determine its composition, using a Jasco-6000 FTIR spectrometer in transmission mode. To acquire the spectra, about 2 mg of powder was mixed with 200 mg of KBr to produce a pellet for analysis.

The morphology of the TBC powder was analyzed with a high-resolution Zeiss Sigma 300 VP field-emission scanning electron microscope (FE-SEM, Carl Zeiss AG) in secondary electron mode. To avoid charge accumulation, the powder was affixed to a double-sided carbon tape on aluminum stubs and then sputter-coated with 10 nm gold (CCU-010 LV, Safematic) before analysis. The surface charge of the powder was measured with a Dynamic Light Scattering instrument (NanoZS90), by using a suspension of the milled powder with a concentration of 1 mg/ml.

The TBC surface area was estimated through $N_2$ gas adsorption following a Brunauer-Emmett-Teller method (BET), by using a Surfer Thermo Fisher Scientific instrument. The dimensions of the pores were determined with mercury porosimetry measurements, using two different units namely, the Pascal 140 unit to measure pores with diameters between 3.5 and 100 mm and achieved a pressure of up to 400 kPa, and the Pascal 240 unit to measure micro-mesoporosity with diameters between 0.008 and 10 mm, achieving a maximum pressure of 200 MPa. The sample was outgassed under vacuum at 200 °C for 1 h prior to testing. The $N_2$ adsorption-desorption isotherm curves were measured with a Micrometric TriStar II Plus equipment, after outgassing at 30 °C.

From the BET surface area, the size of the powder was estimated; more specifically the equivalent spherical diameter ($d_{BET}$) was calculated with the following equation (Scalera et al., 2013):

$$d_{BET} = \frac{6}{\rho SS} \tag{1}$$

where $\rho$ is the density of the powder, and SS stands for its surface area. A density value of 3.156 g/cm$^3$, which is the theoretical density of stoichiometric hydroxyapatite, was used.

### 2.3. Adsorption experiments

The capacity of the TBC to adsorb TRA and VNF was evaluated through batch adsorption assays performed in different aqueous matrices: (1) water, (2) non-saline wastewater (without sea salts); (3) saline wastewater with 7.5 g/L of sea salts; and (4) saline

wastewater with 12 g/L of sea salts. These salt concentrations are regarded as high salinity levels, according to the saline water classification described elsewhere ("The Chemistry of Processes in the Hydrosphere," 2007).

The assays were carried out in 10 mL flasks containing 5 mL of the aqueous matrix and 10 mg of the TBC powder. TRA and VNF were added, individually or combined, to each flask, to attain an initial concentration of 10 mg/L for each pollutant. All flasks were incubated at 30 °C, with continuous shaking at 70 rpm for 24 h. Each condition was tested in triplicate.

During the assay, liquid samples (ca. 0.2 mL) were collected at distinct contact times (0 min, 20 min, 40 min, 60 min, 90 min, 3 h and 24 h). The samples were centrifuged (14500 rpm, 10 min, at room temperature) to separate the solid residues from the liquid fraction, and the resulting supernatants were collected for further chromatographic analysis.

The composition of the synthetic wastewater used was as follows: sodium acetate ($NaCH_3COO$, 0.48 g/L), magnesium sulfate ($MgSO_4.7H_2O$, 0.08 g/L); potassium chloride (KCl, 0.03 g/L); disodium phosphate ($Na_2HPO_4$, 0.06 g/L); monopotassium phosphate ($KH_2PO_4$, 0.03 g/L); ammonium chloride ($NH_4Cl$, 0.18 g/L). In coastal WWTPs, the wastewater salinity can vary throughout the day due to the seawater intrusion events, thus an appropriate mass of seawater salts (Red Sea ®) was added to the saline matrices to achieve initial sea salt concentrations of 7.5 g/L and 12 g/L.

### 2.4. Analytical methods

An Ultimate3000 Dionex UHPLC (Thermo Scientific) combined with an ultra-high resolution quadruple time of flight (UHR-QqTOF) mass spectrometer (Impact II, Bruker Daltonics, Germany) equipment was used to estimate the VNF and TRA concentrations. Electrospray ionization was used with the following acquisition parameters: capillary voltage, 2.5 kV; end plate offset, 500 V; charging volt, 600 V; nebulizing gas pressure, 2.5 Bar; dry gas ($N_2$) flow, 8.0 L/min; probe gas temperature, 300 °C; dry heater temperature, 240 °C. The tune parameters were as follows: ion energy, 3 V; collision energy, 10 V; transfer time, 82.5 μs; collision RF, 500 Vpp; pre-pulse storage, 5.0 μs; low mass, 50 mz. The scan mode implemented broadband collision-induced dissociation (bbCID) was set for a positive ionization. The acquisitions were performed with an *m/z* range from 30 to 1000, and a spectra rate of 8 Hz. Data was processed in the Compass Data Analysis software (version 5.0).

The chromatographic separation was performed using a Chiral Stationary Phase (CSP) column namely Astec Chirobiotic™ V, 5 μm (150 mm length × 2.1 mm internal diameter) (SUPELCO Analytical, Sigma-Aldrich), and a mobile phase composed of ethanol/10 mM aqueous ammonium acetate buffer (92.5/7.5, v/v), with pH adjusted to 6.8 (Ribeiro et al., 2014). The elution was performed in isocratic mode at a flow rate of 0.32 mL/min, a run time of 15 min, and an injection volume of 5 μL.

The quantification of TRA and VNF in the different aqueous matrices was performed using the external calibration curve method. Calibration curves were prepared by diluting each pharmaceutical standard solution in each aqueous matrix used in batch experiments. A set of eight different standard concentrations of TRA and VNF were used for the calibration curves: 0.5; 1; 2; 4; 6; 8; 10 and 12 mg/L. The pharmaceutical concentration estimated for each sample was the result of duplicate injections.

The applied chromatographic method allowed the enantiomeric separation of VNF, but not for all tested conditions. The quantification of the (*S*)–VNF and (*R*)-VNF enantiomers was only possible when the VNF was present alone in the aqueous matrix composed of water. In the remaining three aqueous matrices, the presence of salt ions and other wastewater constituents hindered an accurate separation of the VNF enantiomers, caused by the loss of the column resolution. Similarly, the mixture of VNF and TRA in the four different aqueous matrices prevented a precise enantiomeric separation of VNF.

### 2.5. Data analysis

The adsorption capacity ($q_t$) and the adsorption removal efficiency (R%) were estimated according to the following equations, respectively:

$$q_t\left(\frac{mg}{g}\right) = \frac{(Ci - Cf) * V}{m} \tag{2}$$

$$Adsorption\ removal\ efficiency\ (\%) = \frac{(Ci - Cf)}{Ci} * 100 \tag{3}$$

where $q_t$ is the amount of pharmaceutical adsorbed per mass of sorbent (mg/g), $C_i$ and $C_f$ are the initial and final pharmaceutical concentrations (mg/L), V is the solution volume (L) and m is the sorbent mass (g).

The enantiomeric fraction was determined using the following equation:

$$EF = \frac{C\ (S)}{(C\ (S) + C(R))} \tag{4}$$

where C(*S*) and C(*R*) represent the concentrations of the (*S*) and (*R*) enantiomers of the chiral pharmaceuticals.

### 2.6. Statistical analysis

Data on the experimental $q_t$ and removal efficiency were analyzed using One-way ANOVA and subsequent Tukey's post-test, with $p < 0.05$ defined for significance. Student's t-test was performed to evaluate the significance of the differences observed for each pharmaceutical (individually or in a mixture) within each type of matrix. Normal distribution was verified with the Shapiro-Wilk test ($p > 0.05$). For data not presenting a normal distribution, the non-parametric Kruskal-Wallis test was performed. The statistical analysis was done using the SPSS program (SPSS Inc., Chicago, IL version 26.0).

## 3. Results and discussion

### 3.1. TBC characterization

As the material source and/or the pyrolysis conditions may lead to BC with different characteristics (Piccirillo, 2023), the TBC powder characterization was performed. The SEM methodology was used to assess the morphology of the TBC powder. Fig. 1A shows small particles aggregated into larger ones, with the formation of some voids in the powder structure, marked with red circles. Moreover, at higher magnification (Fig. 1B and C), it can be seen that the individual particles are of nanometric size, between 30 and 60 nm, making the material nanostructured. SEM analysis also revealed that the material presented a rough surface morphology.

The surface area and the pore size distribution are important parameters to assess the adsorption material's capacity for pollutants. The TBC surface area was 100.67 $m^2/g$ (Table 1), which is comparable to that of other animal-derived BC (Jia et al., 2018; Medellín-Castillo et al., 2014; Muretta et al., 2022; Piccirillo, 2023). Using equation (1), an equivalent spherical diameter ($d_{BET}$) of about 32 nm was obtained, therefore, in agreement with what was observed from the SEM images (Lightfoot, 1998). The pyrolysis process at high temperatures such as 1000 °C promotes a higher release of gases during the process that, in turn, leads to obtaining materials with higher surface area (Côrtes et al., 2019). This behavior is the opposite of what happens to calcium phosphate-based ceramics whenever they are heated in air/reactive atmosphere, when sintering normally occurs, accompanied by a decrease of the surface area (Piccirillo et al., 2015). Even though large surface areas are known to confer high pollutant adsorption capacity to adsorbent materials, the surface chemical composition of BC-based materials is also a very important feature. Indeed, the presence of different functional groups surely plays a role in the efficiency of the adsorption process (Medellín Castillo et al., 2023). This is because such groups that exist on the surface of the BC materials have the capability of interacting with a wide range of molecules (Piccirillo, 2023).

Fig. 2A shows the $N_2$ adsorption-desorption curve for the TBC powder. It is a type V isotherm typical of a relatively weak adsorbent-adsorbate interaction. The small hysteresis loop indicates some capillary condensation in the mesopores (dimensions below 50 nm). The hysteresis loop shape is H4 type, often associated with narrow-slit pores. Fig. 2B shows the distribution of the dimensions of the pores (red histograms, right Y axis) and the cumulative pore volume (blue curve, left Y axis). Regarding the pore dimensions, a bimodal distribution is observed, with dimensions within the order of nanometres and microns, respectively. Indeed, data indicate the presence of pores with dimensions between about 8 and 80 nm (maximum relative volume for 16 nm). On the other hand, a wider distribution between about 0.1 μm and 80 μm was detected for higher dimensions. Considering the morphology of the TBC material observed by SEM analysis, it is likely that the smaller pores (mesopores) are those within the particles themselves, while the larger ones are due to the aggregation into bigger particles and the consequent voids formed between them (Fig. 1A, red circles). The total pore volume was 575.2 $mm^3/g$ (Table 1), comparable with those of other BC-type materials (Acosta-Herrera et al., 2021; Cazetta et al., 2018). The mesopore volume (pores with dimensions between 2 and 50 nm) was 137.0 $mm^3/g$ (Table 1). The porosimeter analysis indicated the presence of nanometric pores which maximize the contact between the TBC powder and the adsorbate, allowing the adsorbate penetration inside it. Indeed, pore filling is considered one of the key mechanisms occurring in adsorption processes (Puga et al., 2022).

FTIR spectroscopy was used to investigate the composition and the surface functional groups of the TBC material, and the spectrum is shown in Fig. 3. It can be seen that the signals associated with the $PO_4$ group are present at 1091, 1036, 950, 602, and 563 $cm^{-1}$ (Piccirillo et al., 2017). A wide peak at about 3443 $cm^{-1}$ is attributed to the OH group present in the hydroxyapatite (Côrtes et al.,

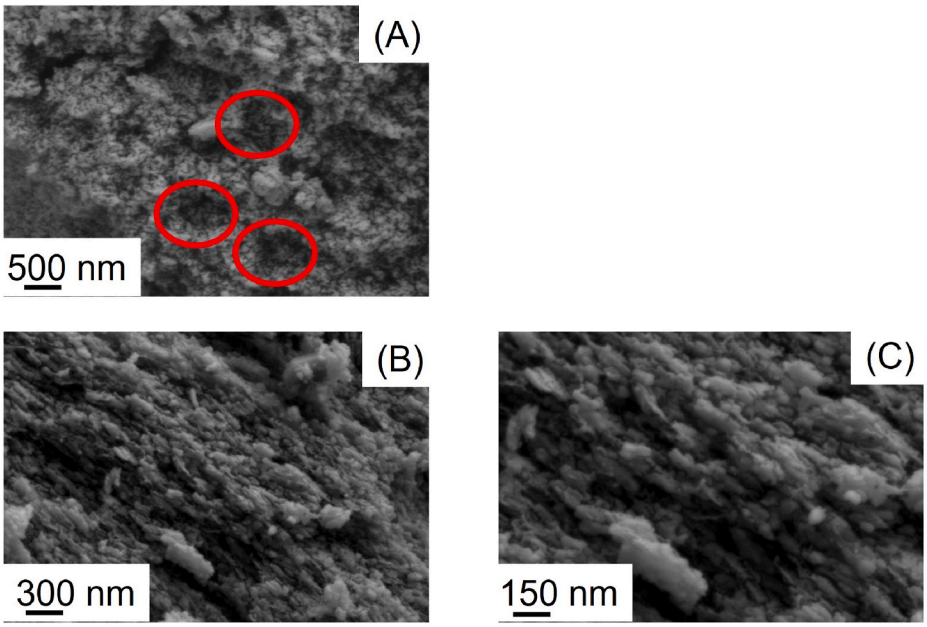


**Fig. 1.** SEM micrographs of the TBC powder at various magnifications (A–C). Red circles in (A) indicate the formation of voids in the powder structure. (For interpretation of the references to colour in this figure legend, the reader is referred to the Web version of this article.)

**Table 1**
Specific surface area, total pore volume and mesopore volume for the TBC powder.

| Parameter | Value |
|---|---|
| Specific surface area ($m^2/g$) | 100.67 |
| Total pore volume ($mm^3/g$) | 575.2 |
| Mesopore volume ($mm^3/g$) | 137.0 |

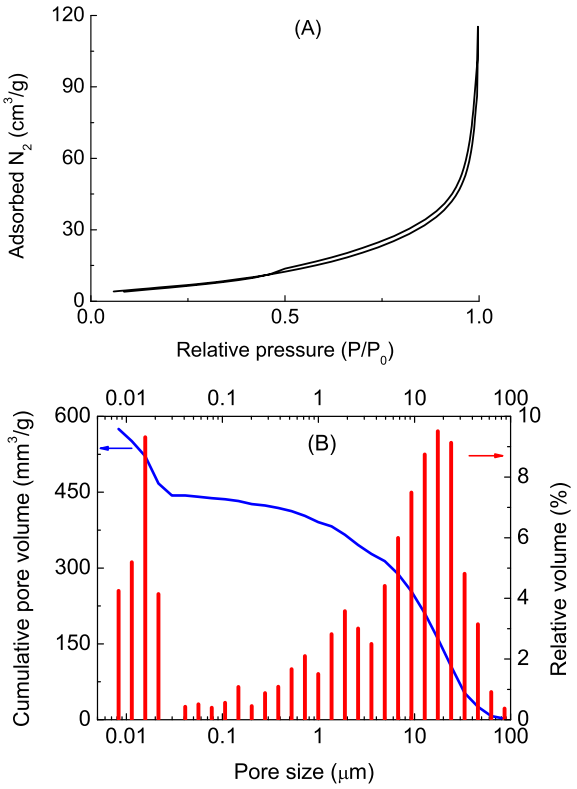


**Fig. 2.** $N_2$ adsorption/desorption isotherm curve (A); the cumulative pore volume (blue line), and the histogram of the relative volume (red columns) as a function of the TBC powder pores size (B). (For interpretation of the references to colour in this figure legend, the reader is referred to the Web version of this article.)

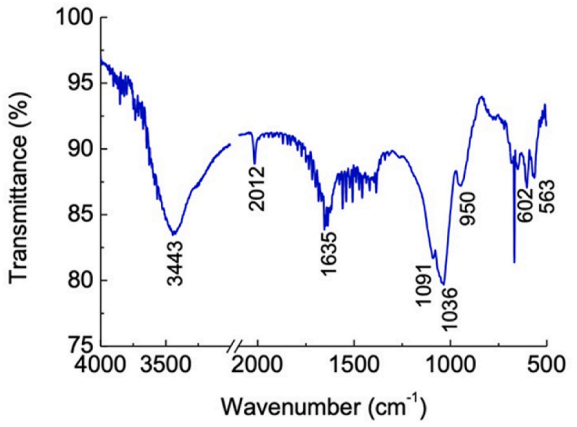


**Fig. 3.** FTIR spectrum of TBC material.

2019). It is worth mentioning that for other BC materials prepared in similar conditions, this band was much less intense (Alkurdi et al., 2020), as with graphite formation, the hydroxyapatite proportion became smaller. This does not seem to be the case in the present work, however; as already mentioned above, different starting materials can result in BC with different characteristics (Park et al., 2015; Reynel-Avila et al., 2015; Wang et al., 2020). Similarly, the wide band at 1635 $cm^{-1}$, associated with the C–O bond, was reported to be less intense for BC-derived from sheep bone prepared at temperatures above 800 °C (Alkurdi et al., 2020). The sharp peak at 2012 $cm^{-1}$ was previously reported for BC-type powders and it is due to the formation of the $NCN^{2-}$ ion that takes place during the pyrolysis, due to the reaction/degradation of the proteins present in the bones (Piccirillo et al., 2017).

The surface charge of the TBC powder, measured by DLS spectroscopy, was -12.1 mV, which is in agreement with already published data (Alkurdi et al., 2019). In some cases, however, even more negative values were measured for BC-type materials prepared at similar pyrolysis temperatures (Alkurdi et al., 2020; Guo et al., 2022). These negative charges are likely due to the presence of oxygen-containing groups, such as phosphates or OH (often deprotonated).

### 3.2. TBC adsorption capacity

The efficiency of the TBC to remove two pharmaceuticals, TRA and VNF, was assessed. The selected pharmaceuticals are molecules that can be good models for adsorption studies due to the different kinds of molecular interactions that could be established with the adsorption material. Additionally, the environmental occurrence of TRA and VNF has been often reported (Castaño-Ortiz et al., 2024; Kodešová et al., 2024; Vaudreuil et al., 2024); thus, innovative methods to be applied in WWTPs to avoid their release are of major importance.

The efficiency of the TBC for the adsorption of the target pollutants was evaluated when the pharmaceuticals were supplied individually or in a mixture, using aqueous matrices with different chemical complexity, including synthetic wastewater with different levels of salinity.

Fig. 4 shows the amount of TRA and VNF adsorbed per unit of material ($q_t$) as a function of time in different conditions, while Table 2 shows the experimental $q_t$ reached after 24 h of contact time, as well as the overall removal efficiency in each condition. In all cases, most of the adsorption of pharmaceuticals onto the TBC takes place in the first 3–4 h of contact (Fig. 4). Afterward, the adsorption continued to occur, but at a smaller rate. In most cases, when the aqueous matrix was composed of saline wastewater, the

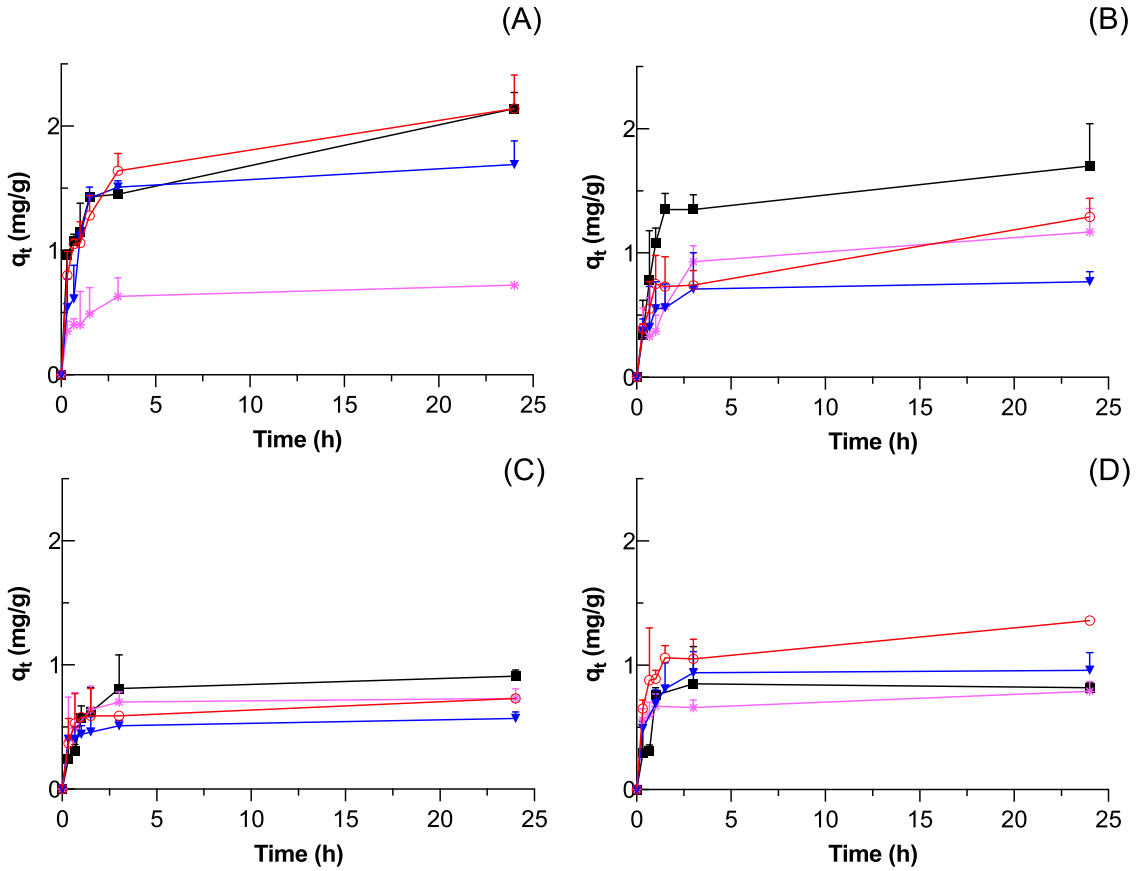


**Fig. 4.** The adsorption capacity ($q_t$) of the TBC powder for each pharmaceutical, namely TRA and VNF when present alone (A and B, respectively), or as a mixture (C and D for TRA and VNF), in the different types of aqueous matrices. Adsorption assays were performed in four different aqueous matrices, namely in water (■), non-saline wastewater (○), saline wastewater with 7.5 g/L of sea salts (▼), and saline wastewater with 12 g/L of sea salts (○).

**Table 2**
**Experimental** $q_t$ (mg/g) and TBC adsorption efficiency (%) for VNF and TRA (alone and in a mixture) by the end of 24 h of contact time.

| Type of aqueous matrix | Experimental $q_t$ (mg/g) | | | | Adsorption efficiency (%) | | | |
|---|---|---|---|---|---|---|---|---|
| | Pharmaceuticals alone in the aqueous matrix | | Pharmaceuticals as a mixture in the aqueous matrix | | Pharmaceuticals alone in the aqueous matrix | | Pharmaceuticals as a mixture in the aqueous matrix | |
| | VNF | TRA | VNF | TRA | VNF | TRA | VNF | TRA |
| Water | 1.70 ± 0.34$^{a}$ | 2.14 ± 0.13$^{a}$ | 0.82 ± 0.04$^{a}$ | 0.91 ± 0.05$^{a}$ | 35.97 ± 7.20$^{a}$ | 43.10 ± 2.59$^{a}$ | 16.62 ± 0.90$^{ns}$ | 17.29 ± 0.87$^{a}$ |
| Non-saline wastewater | 1.29 ± 0.15$^{ab}$ | 2.14 ± 0.27$^{a}$ | 1.36 ± 0.02$^{b}$ | 0.73 ± 0.02$^{ab}$ | 28.84 ± 3.36$^{ab}$ | 39.45 ± 5.02$^{a}$ | 29.52 ± 0.49$^{ns}$ | 14.82 ± 0.37$^{ab}$ |
| Wastewater w/7.5 g/L of sea salts | 0.77 ± 0.08$^{b}$ | 1.69 ± 0.19$^{a}$ | 0.96 ± 0.14$^{a}$ | 0.57 ± 0.05$^{b}$ | 17.77 ± 1.07$^{b}$ | 29.32 ± 3.27$^{b}$ | 23.93 ± 6.67$^{ns}$ | 12.46 ± 1.15$^{b}$ |
| Wastewater w/12 g/L of sea salts | 1.17 ± 0.19$^{ab}$ | 0.72 ± 0.03$^{b}$ | 0.79 ± 0.08$^{a}$ | 0.73 ± 0.08$^{ab}$ | 22.37 ± 3.65$^{b}$ | 14.67 ± 0.61$^{c}$ | 16.75 ± 1.74$^{ns}$ | 14.10 ± 1.48$^{b}$ |

Results are expressed as means ± SD; Means with different letters in the same column differed significantly according to the Tukey post-test and non-parametric Kruskal-Wallis test ($p < 0.05$).

maximum adsorption (i.e. TBC saturation) was reached before the first 24 h, whilst for non-saline wastewater, the adsorption of the pharmaceuticals onto TBC slowly continued to occur until the end of the experiment.

### 3.2.1. *Single pharmaceutical adsorption to TBC*

Concerning the TRA adsorption onto TBC, whenever this pharmaceutical is the sole pharmaceutical in the aqueous matrix, the highest adsorption capacity (ca. 2.1 mg/g) was registered in the aqueous matrices composed by only water and non-saline wastewater (Fig. 4A). Although in saline wastewater with 7.5 g/L sea salts, the TBC adsorption capacity for TRA was lower (ca. 1.7 mg/g), it was not significantly different from those obtained in water and non-saline wastewater. Nevertheless, if saline wastewater with 12 g/L sea salts is used, the TBC adsorption capacity is significantly lower (about ¼ of the highest value – 0.7 mg/g). This indicates that a high content of salts in the aqueous matrix decreased the TBC adsorption for TRA probably due to some competing effects between the salt ions and some molecular groups of the pharmaceutical compounds for the available binding sites in the material. This phenomenon is described as the "squeezing-out effect", and occurs when cations present in the aqueous matrix exhibit a superior binding affinity for the adsorbent compared to the adsorbates, resulting in the displacement of adsorbates from the BC surface. During this phenomenon, cations in the solution can compress the electric double layer on the adsorbent surface, thus compromising the adsorption of micropollutants (Wu et al., 2020). A similar trend was reported by Maged et al. (2021), that verified that the activated biochar adsorption efficiencies for levofloxacin were compromised when NaCl was present in the solution, attributing this decline to the squeezing-out effect.

When VNF was the sole pharmaceutical in the aqueous matrix, the highest adsorption onto TBC was achieved in the matrix consisting only of water (Fig. 4B), although its experimental $q_t$ value was lower than that obtained for TRA in the same condition (1.7 vs. 2.1 mg/g, respectively). In this specific condition, it was also possible to follow the removal of the (*S*) and (*R*) enantiomers of VNF. Similar adsorption profiles were obtained for (*S*)–VNF and (*R*)-VNF. With the EF estimation for each enantiomer, it is possible to provide relevant insights into the fate and risk of the chiral compounds in both abiotic and biotic processes. Indeed, the EF over time was 0.55 for (*S*)–VNF and 0.45 for *(R)*-VNF (Fig. 5), indicating that the adsorption of VNF by the TBC material was a non-enantioselective process and, therefore, no preferential adsorption of (*S*)–VNF over (*R*)-VNF occurred. As the TBC preparation consists of a high-temperature treatment (i.e. pyrolysis process), a chiral structure was not expected, and, thus, enantioselective

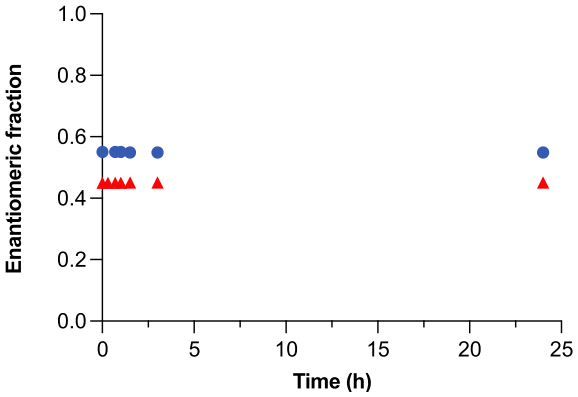


**Fig. 5.** Enantiomeric fraction (EF) variation for each enantiomer of VNF, namely (S)–VNF (●) and (R)-VNF (▲). The EF means and respective standard deviations were estimated for each contact time when VNF was supplied individually, and the aqueous matrix was water. SD bars are shown in the graph, but they are too small to be visible.

pharmaceutical adsorption was highly unlikely.

When the aqueous matrices were non-saline or saline wastewater, the experimental $q_t$ values for VNF were lower than those obtained in the water-based matrix, and enantiomer separations in the chiral column were no longer possible due to the lack of column resolution, probably due to the presence of salts and other ions in matrices with higher chemical complexity (Table 2). However, for VNF, the lowest $q_t$ was registered for saline wastewater with 7.5 g/L of salts, while no significant differences were observed if the aqueous matrix was water, non-saline wastewater, or wastewater with 12 g/L sea salts. This was unexpected given the lower $q_t$ obtained for TRA when solely present in a wastewater matrix with 12 g/L salts, as in this scenario the higher salt concentration affected the TBC adsorption capacity to a greater extent. While it is challenging to attribute a specific cause for this variation, it may be likely related to the signal enhancement during the chromatographic analysis due to the presence of high salinity levels.

### 3.2.2. Pharmaceuticals adsorption in a mixture

Whenever the aqueous matrix contained simultaneously TRA and VNF, often lower experimental $q_t$ values were registered in comparison to those observed with only one pollutant in the aqueous matrix. This was partly expected, as in total the initial concentration of pharmaceuticals was 20 mg/L, i.e. double the amount. In such conditions, the TBC capacity to remove TRA was not significantly different from that observed in water, non-saline wastewater, or saline wastewater with 12 g/L sea salts (Fig. 4C). However, experimental $q_t$ values obtained for wastewater with 7.5 g/L sea salts were significantly lower than those obtained in water ($p < 0.05$), although not significantly different from those in non-saline wastewater or wastewater with the highest sea salt concentration.

The adsorption profile of VNF whenever this pharmaceutical coexisted with TRA in the aqueous matrix was different from that obtained when VNF was the sole pharmaceutical (Fig. 4D). Here, the TBC powder showed a superior capacity for removing VNF in non-saline wastewater (1.36 mg/g) and wastewater with 7.5 g/L sea salts (0.96 mg/g), in comparison to its capacity to remove VNF present as the sole pharmaceutical in the aqueous matrix (Table 2). Nevertheless, whether the adsorption experiments of the VNF were carried out either solely or in a mixture, the *t*-test showed no statistical differences in the TBC adsorption capacities if non-saline wastewater ($p = 0.513$) or wastewater with 7.5 g/L sea salts ($p = 0.591$) were used as aqueous matrices. On the other hand, the TBC adsorption capacity for VNF was lower when the highest sea salt concentration was used (0.79 mg/g). In this condition, $q_t$ values obtained in the non-saline wastewater differed significantly from the other three conditions ($p < 0.05$). It is worth mentioning that whether the VNF was supplied alone or in a mixture, in the aqueous matrix containing the highest sea salt concentration, the statistical analysis indicated that the $q_t$ achieved in such conditions is significantly different ($p < 0.05$). This indicates that increasing the complexity of the aqueous matrix composition together with the combination of pharmaceuticals in the matrix compromised the TBC adsorption effectiveness, although the TBC was still able to adsorb both pharmaceuticals. Moreover, in all experiments conducted with both pharmaceuticals simultaneously present in the aqueous matrix, after 3 h of contact time, the adsorption capacity reached a plateau (Fig. 4C–D).

In the present study, the pharmaceuticals were supplied each at concentrations of 10 mg/L, which were much higher than those presently reported in the WWTP effluents or environmental aqueous matrices (>100 ng/L and >200 ng/L for VNF and TRA, respectively) (Kodešová et al., 2024; Park et al., 2018; Rúa-Gómez and Püttmann, 2012). This was done because the main aim of this study was to evaluate the effect of the different salinity levels on the capacity of the TBC powder for the adsorption of target pharmaceuticals; hence higher concentration values were considered, to better highlight possible differences and/or interferences.

The adsorption experiments revealed that the presence of salt ions in the aqueous matrix can affect the TBC adsorption capacity for the target pharmaceuticals in different ways. Ionic pollutants can establish interactions with the ions, leading to possible changes in their charge; this, in turn, will allow for different interactions with the sorbent material and, thus, different adsorption efficiencies (Xiang et al., 2019; Zhang et al., 2015). This can also be observed, although to a minor extent, with polar molecules or those with delocalized electron distribution, like benzene rings or their derivatives (Lamichhane et al., 2016). The interactions with charged ions can cause changes in the electron distribution and, hence, affect the adsorption processes. Competitive mechanisms can also occur when ions in solution compete with the target molecules for binding sites on the solid adsorption material, ultimately reducing the efficiency of the overall adsorption process (Goh et al., 2022). Considering in particular BC-type materials, they have distinct removing mechanisms for ions (i.e., $Na^+$, $Mg^{2+}$, etc.) and organic molecules. For metallic ions, an ionic exchange takes place with the $Ca^{2+}$ ion of the phosphate phase of the BC; for organic molecules, on the other hand, surface adsorption predominantly occurs (Piccirillo, 2023). In the present study, it appears that the interactions between the TBC and the target pharmaceuticals are weakened by the presence of ions, particularly those from sea salts in wastewater. This effect was observed for TRA and became more pronounced at higher salinity levels (Fig. 4A).

The adsorption assays revealed that the simultaneous adsorption of TRA and VNF onto TBC was faster at the beginning (first 3 h) (Fig. 4A–D), with the adsorption process continuing to occur over time but at a slower rate. This type of behavior suggests that most of the adsorption of VNF and TRA may occur on the TBC external surface, as the accessibility of these two organic molecules for the binding sites is high (Reynel-Avila et al., 2015).

## 3.3. Effect of different aqueous matrices on the TBC removal efficiency

The overall TBC removal efficiencies for TRA and VNF, alone or in a mixture, after 24 h are shown in Table 2. For TRA, the highest removal efficiencies were observed in water (43.1%), and non-saline wastewater (39.4%), showing no significant differences between them. In general, the salts' presence in the wastewater decreased the TBC removal capacity for TRA. The adsorption efficiency was significantly lower in wastewater with 7.5 g/L, but the inhibitory salt effect was even more pronounced in wastewater with 12 g/L sea salts (29.3% *vs* 14.7% of TRA removal).

Regarding the adsorption capacity for VNF, whenever it is the only pharmaceutical in the aqueous matrix, the highest removal efficiencies were recorded in water (36.0%). If wastewater was used as aqueous matrix, the TBC adsorption efficiency for VNF decreased, with a more pronounced decrease when saline wastewater was used: 28.8% of removal in non-saline *vs* 17.8% and 22.4% in saline wastewater with 7.5 and 12 g/L sea salts, respectively.

When assays were performed with both pharmaceuticals in the aqueous matrix, TRA exhibited much lower adsorption onto TBC in water, non-saline wastewater, and 7.5 g/L saline wastewater, with removal efficiencies ranging from 12.5 to 17.3%. In wastewater with 12 g/L seawater salts, on the other hand, the removal efficiency was much closer to that obtained for TRA as the sole pharmaceutical in the aqueous matrix (around 14%).

The TBC capacity for removing VNF in a mixture with TRA was very similar, regardless of the aqueous matrix ($p > 0.05$). Nevertheless, when both pharmaceuticals co-exist in the aqueous matrix, the TBC presented lower removal efficiencies for VNF in comparison to its capacity to remove the VNF if it is the sole pharmaceutical in the aqueous matrix. This effect, however, was not so pronounced as that observed for TRA. The most pronounced effect was observed with only water as the aqueous matrix, as the overall VNF removal was less than half than for VNF alone (about 16.6 *vs* 36.0%). For the other types of aqueous matrices, higher removal efficiencies were recorded in non-saline wastewater (29.5%), and wastewater with 7.5 g/L sea salts (23.9%). However, the TBC showed a lower adsorption capacity for VNF in wastewater with 12 g/L sea salts (16.8%).

Comparing the efficiency of the TBC for adsorbing each of the pharmaceuticals, overall, it has a higher capacity to adsorb TRA than VNF, indicating a higher affinity between TBC and TRA. However, when TRA and VNF are simultaneously present in the aqueous matrix, the adsorption of the two molecules is similar, i.e., no preferential adsorption of TRA was observed. Nevertheless, TBC removal efficiencies for each pollutant in the mixture were lower than the ones for each pollutant individually in the matrix, meaning that the presence of multiple adsorbates in the matrix compromised the adsorption of each other. In a previous study, the adsorption of VNF and fluoxetine using marine seaweed as an adsorption material revealed that the presence of both pharmaceuticals in the same matrix did not compromise the adsorption of each pharmaceutical. Also, no differences were found between the $q_t$ values in the adsorption studies conducted using each pharmaceutical individually, or in a mixture (Silva et al., 2019).

Moreover, it is interesting to note that the sum of the adsorption capacity for each pharmaceutical in the mixture was higher than that obtained for the pharmaceuticals when present solely in the aqueous matrices, both in non-saline and saline wastewater (Table 2). This scenario, although not common, was previously reported (Yadav et al., 2021) [and references therein]. This can be explained considering that the interactions between different molecules lead to higher affinity towards the adsorption material. Table 3 lists the adsorption efficiency and surface area of different adsorbent materials for TRA and VNF adsorption that have been explored so far. Although the adsorption of these target pollutants has been previously reported for other adsorption materials, the employment of a BC-type material is reported here for the first time.

In the case of TRA, biochar and lignin-nanocellulose composites were already tested for its adsorption capacity (Agustin et al., 2023; Wurzer et al., 2023), whilst vermiculite and biochar were used to adsorb VNF (Puga et al., 2022; Silva et al., 2018). Moreover, the referred studies were performed in water or synthetic wastewaters that do not contain salts in their composition, a feature that should be taken into consideration if a broad application of the materials is envisaged.

Rúa-Gómez et al. (2012) tested different types of activated carbon for TRA adsorption, all presenting higher adsorption efficiencies

**Table 3**
Adsorption efficiency and BET surface area of different adsorbent types for the target pharmaceuticals.

| Pharmaceutical compound | Adsorbent type and process parameters | BET surface area ($m^2/g$) | Adsorption capacity (mg/g) | Aqueous matrix | Reference |
|---|---|---|---|---|---|
| TRA | Lignin nanoparticle nanocellulose cryogels. | n.a[a] | 150 | Water | Agustin et al. (2023) |
| | Activated carbon Carbopal AP. | 899 | 84 | Water | Rúa-Gómez et al. (2012) |
| | Green alga *Scenedesmus obliquus*. NaOH modification. | n.a[a] | 140 | Wastewater | Ali et al. (2018) |
| | Tuna bone char. $N_2$ atmosphere. 1000 °C. | 101 | 2.14 | Water | This study |
| | | | 2.13 | Non-saline wastewater | |
| | | | 1.69 | Saline wastewater w/ 7.5 g/L sea salts | |
| | | | 0.72 | Saline wastewater w/ 12 g/L sea salts | |
| VNF | Eucalyptus biochar. 500 °C. Without gas supply. | 335 | 2.60 | Wastewater | Puga et al. (2022) |
| | Raw vermiculite. | 21 | 5.80 | Water | Silva et al. (2018) |
| | Non-activated carbon: paper mill sludge (PS800-150). $N_2$ atmosphere, 500 °C. | 209 | 8.50 | Water | Calisto et al. (2015) |
| | Tuna bone char. $N_2$ atmosphere, 1000 °C. | 101 | 1.70 | Water | This study |
| | | | 1.29 | Non-saline wastewater | |
| | | | 0.77 | Saline wastewater w/ 7.5 g/L sea salts | |
| | | | 1.17 | Saline wastewater w/ 12 g/L sea salts | |

[a] Not available.

compared to the ones obtained for the TBC. However, it is important to emphasize that, unlike activated biochars, TBC is generated from the pyrolysis of tuna bones but no further chemical treatment nor activation procedures were made. In contrast, activated carbons are usually subjected to chemical and physical treatments during the production process which largely enhance their adsorption capacity, thus explaining their higher removal efficiencies, compared to the TBC (Cha et al., 2016). Although these treatments improve the adsorption performance of the materials, often toxic chemicals are applied (i.e. acids); the impact of their preparation on the environment is, therefore, higher compared to pyrolysis, the only process used for the TBC preparation.

On the other hand, VNF adsorption by an agroforestry biochar material showed adsorption efficiencies relatively lower compared to the TBC (Puga et al., 2022). In fact, when eucalyptus biochar was used to adsorb VNF and other two pollutants, $q_e$ values of 0.58 mg/g in real wastewater were obtained. In comparison to eucalyptus biochar, the TBC adsorption capacity for VNF when combined with TRA was twice as high in non-saline wastewater ($q_t$ of 1.36 mg/g) and slightly higher in water and saline wastewater with 7.5 g/L sea salts (experimental $q_t$ of 0.82 and 0.96 mg/g, respectively). Like TBC, the biochar material used in the latter study did not undergo any activation treatment to improve its adsorption capacity, which could explain the similarity of its adsorption capacity to that of TBC. Nevertheless, it should be noted that the composition of the real wastewater in the adsorption assays with eucalyptus biochar was not provided, so it is not possible to ascertain the potential influence of salts in the adsorption process. However, as referred to by the authors, organic matter, complex pollutants and ions often co-exist in wastewater.

### *3.4. Surface interactions between TBC and target pharmaceuticals*

VNF and TRA have closely related chemical structures, sharing both hydrophilic and hydrophobic moieties. Their hydrophilic nature is due to the presence of the amino and hydroxyl groups that can establish hydrogen bonds with the TBC material, while their hydrophobic nature is related to the existence of aromatic rings in their structures. VNF and TRA, in their hydrochloric form, have similar pKas (14.4 and 13.8, respectively) and were present in their cationic form on the aqueous matrices, as the pH measured in the assays was of ca. 7, which is below their pKa. This allows for electrostatic interactions to be established between the negative surface charge of the TBC (**section 3.1**) and the positive charges of the pharmaceuticals, thus maximizing the interaction between the pharmaceutical and the TBC powder. The TBC surface charge was also measured with the powder in the different matrices, to assess whether different salinity levels affected it or not. Results showed that in all environments TBC kept its negative charge, although some small differences were observed (between −3 and −9 mV). Compared to conventional biochars, i.e. materials of vegetable origin, only consisting of carbon, these hydrogen interactions may be stronger in the TBC material due to the presence of the phosphate phase. Indeed, the $PO_4$ groups present in the hydroxyapatite of the TBC can establish hydrogen bonds with the atoms of the hydroxyl groups of the pharmaceuticals. Fig. 6 illustrates some of the main mechanisms that can be involved in the adsorption of the target pharmaceuticals onto TBC. Besides the electrostatic interaction that is highly expected to occur between TBC and the target pharmaceuticals, there are other types of interactions that can also happen for organic compounds, including hydrogen bonds, pore filling, partitioning, hydrophobic effects or by π–π electron dispersion interaction, with the aromatic rings of the pharmaceuticals and the aromatic rings of the carbon phase of the TBC (Reynel-Avila et al., 2015). It is worth mentioning that the adsorption of this type of organic molecules from aqueous matrices on carbon-based materials is a complex process and can involve electrostatic and non-electrostatic interactions, as their removal process relies on many parameters, including the properties of the adsorption material, adsorbate, and chemical matrix composition (Sotelo et al., 2012).

Although it is challenging to provide a detailed mechanism, it appears that the presence of other ions in the aqueous matrix has a substantial effect on the interactions between the pharmaceuticals and the adsorption material, although such an effect is different according to the conditions. Results show that the salt ions in wastewater have a detrimental effect on the adsorption of each pharmaceutical alone, but almost no effect or a positive effect is observed when the two pharmaceuticals are tested in a mixture. Additionally, the presence of salt ions also impacts the electrostatic nature and configuration of each pharmaceutical, decreasing their solubility and consequently affecting the adsorption capacity of the BC-type material to the adsorbate. Zhang et al. (2015) performed a stepwise salt increase in the medium concentration and observed a decrease in the adsorption of tetracycline, a positively charged molecule. In this scenario, cations present in the solution competed for binding sites with the tetracycline molecules, decreasing the adsorption of the latter. The authors also observed that the inhibitory adsorption effect was even more pronounced when divalent cations (i.e., $Ca^{2+}$, $Mg^{2+}$, etc.) were present in the solution rather than monovalent ones.

In the present study, the sea salts used for the preparation of the saline wastewaters (Red Sea ®) is mostly composed of divalent magnesium and calcium cations, with lesser content of the trivalent phosphate anion. According to Zhang et al. (2015), it is most likely that the chemical composition of the saline matrices enriched in divalent cations could hinder the TBC adsorption process, as these ions will be preferentially adsorbed by the hydroxyapatite. This may explain the diminished TBC adsorption capacity observed for TRA when tested solely in the aqueous matrix containing 12 g/L sea salts, in comparison to other non-saline matrices. Nevertheless, no data is available regarding possible changes in the pharmaceuticals' solubility in the presence of inorganic ions such as those employed in this study. For VNF, the literature reports changes in its solubility when conjugated with organic acids (Spinelli et al., 2017); for TRA, on the other hand, the solubility in the presence of organic polymers was studied (Sudha et al., 2010). Therefore, this is an aspect that should be further investigated.

## 4. Conclusion

The conversion of tuna fish bones into biochar-like material (Tuna Bone Char, TBC) by pyrolysis at a high temperature (1000 °C) resulted in a powder with a high surface area (100.67 $m^2/g$) and a nanometric structure (particle dimensions of about 30–60 nm), containing both mesopores within the particles and micron scale pores between the agglomerated particles. TBC is a multiphasic

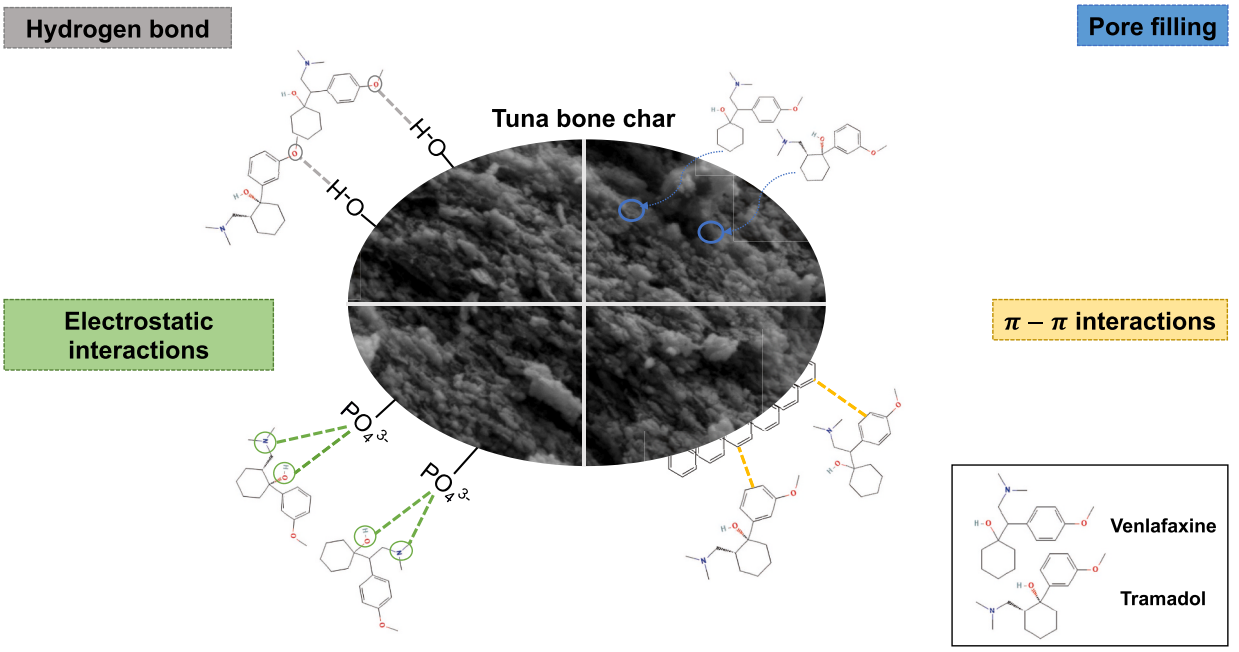


**Fig. 6.** Mechanisms of interaction between TBC and pharmaceuticals TRA and VNF.

material, consisting of both carbon and hydroxyapatite. These characteristics combined with its multiphasic composition categorize TBC within the highly efficient adsorption materials.

The bone-derived material was efficient in removing the two target pharmaceuticals, TRA and VNF in saline and non-saline wastewaters, mimicking a real scenario. Moreover, even in high salinity matrices, the TBC material was effective in adsorbing both pharmaceuticals, with experimental adsorption capacities after 24 h of contact time ranging from 0.77 to 1.70 and 0.72–2.14 mg/g, for VNF and TRA, respectively. The TBC was shown to be effective in simultaneously adsorbing pharmaceuticals when they were combined in the aqueous matrix, an important feature for its potential application; indeed, $q_t$ values of 0.79–0.96 and 0.57–0.73 mg/g were obtained for VNF and TRA.

Overall, the study confirms the potential of bone-derived pyrolyzed materials for the adsorption of pharmaceuticals in different environments. In fact, a material obtained from the by-products of the fisheries and food industries can be transformed into an effective sorbent, in line with the circular economy principles, contributing at the same time to developing alternative environmental remediation processes. Further research should investigate the equilibrium behavior of the systems; different adsorption models should be considered, as well as the thermodynamic features of the processes. A more detailed study on the interactions with the ions present in the wastewaters and their effect on the performance of the material should also be considered.

## CRediT authorship contribution statement

**Catarina Miranda:** Writing – original draft, Methodology, Investigation, Data curation, Conceptualization. **Francesca Scalera:** Writing – review & editing, Writing – original draft, Investigation, Data curation. **Andreana Piancastelli:** Data curation. **Robert C. Pullar:** Formal analysis, Investigation, Validation, Writing – review & editing. **Maria Elizabeth Tiritan:** Writing – review & editing, Writing – original draft, Methodology, Investigation, Data curation. **Clara Piccirillo:** Writing – review & editing, Writing – original draft, Validation, Investigation, Conceptualization. **Paula M.L. Castro:** Writing – review & editing, Writing – original draft, Methodology, Investigation, Funding acquisition. **Catarina L. Amorim:** Writing – review & editing, Writing – original draft, Formal analysis, Data curation, Conceptualization.

## Declaration of competing interest

The authors declare that they have no known competing financial interests or personal relationships that could have appeared to influence the work reported in this paper.

## Data availability

Data will be made available on request.

## Acknowledgments

This work was financed by Norte (2020) through Project 3BOOST (POCI-01-0246-FEDER-181302). The authors thank the CBQF and CIIMAR scientific collaboration under the FCT projects UIDB/50016/2020 and UIDB/04423/2020 + UIDP/04423/2020. C. Miranda thanks the research grant from FCT, Portugal (2020.06577. BD) and POCH, supported by the European Social Fund and MCTES national funds. C. Piccirillo and F. Scalera thank the project PON-SHINE (Potenziamento dei nodi italiani in *E*-RIHS, CIG: Z902D25DCE, CUP: B27E19000030007) funded by Italian MUR for the financial support.

## References

Acosta-Herrera, A.A., Hernández-Montoya, V., Castillo-Borja, F., Pérez-Cruz, M.A., Montes-Morán, M.A., Cervantes, F.J., 2021. Competitive adsorption of pollutants from anodizing wastewaters to promote water reuse. J. Environ. Manag. 293, 112877 https://doi.org/10.1016/j.jenvman.2021.112877.

Agustin, M.B., Lehtonen, M., Kemell, M., Lahtinen, P., Oliaei, E., Mikkonen, K.S., 2023. Lignin nanoparticle-decorated nanocellulose cryogels as adsorbents for pharmaceutical pollutants. J. Environ. Manag. 330, 117210 https://doi.org/10.1016/j.jenvman.2022.117210.

Ahmad, S., Zhang, M., Li, Y., Yang, X., Gao, F., Tang, J., 2023. Pyrolyzed bone char for nitrobenzene adsorption: insight into the physicochemical characterizations and adsorption mechanisms. J. Environ. Chem. Eng. 11, 111597 https://doi.org/10.1016/j.jece.2023.111597.

Ali, M.E.M., Abd El-Aty, A.M., Badawy, M.I., Ali, R.K., 2018. Removal of pharmaceutical pollutants from synthetic wastewater using chemically modified biomass of green alga Scenedesmus obliquus. Ecotoxicol. Environ. Saf. 151, 144–152. https://doi.org/10.1016/j.ecoenv.2018.01.012.

Alkurdi, S.S.A., Al-Juboori, R.A., Bundschuh, J., Bowtell, L., McKnight, S., 2020. Effect of pyrolysis conditions on bone char characterization and its ability for arsenic and fluoride removal. Environ. Pollut. 262, 114221 https://doi.org/10.1016/j.envpol.2020.114221.

Alkurdi, S.S.A., Herath, I., Bundschuh, J., Al-Juboori, R.A., Vithanage, M., Mohan, D., 2019. Biochar versus bone char for a sustainable inorganic arsenic mitigation in water: what needs to be done in future research? Environ. Int. 127, 52–69. https://doi.org/10.1016/j.envint.2019.03.012.

Bangia, S., Bangia, R., Daverey, A., 2023. Pharmaceutically active compounds in aqueous environment: recent developments in their fate, occurrence and elimination for efficient water purification. Environ. Monit. Assess. 195, 1344. https://doi.org/10.1007/s10661-023-11858-7.

Barreiro, J.C., Tiritan, M.E., Cass, Q.B., 2021. Challenges and innovations in chiral drugs in an environmental and bioanalysis perspective. TrAC, Trends Anal. Chem. 142, 116326 https://doi.org/10.1016/j.trac.2021.116326.

Bielen, A., Šimatović, A., Kosić-Vukšić, J., Senta, I., Ahel, M., Babić, S., Jurina, T., González Plaza, J.J., Milaković, M., Udiković-Kolić, N., 2017. Negative environmental impacts of antibiotic-contaminated effluents from pharmaceutical industries. Water Res. 126, 79–87. https://doi.org/10.1016/j.watres.2017.09.019.

Brunson, L.R., Sabatini, D.A., 2014. Practical considerations, column studies and natural organic material competition for fluoride removal with bone char and aluminum amended materials in the Main Ethiopian Rift Valley. Sci. Total Environ. 488–489, 580–587. https://doi.org/10.1016/j.scitotenv.2013.12.048.

Calisto, V., Ferreira, C.I.A., Oliveira, J.A.B.P., Otero, M., Esteves, V.I., 2015. Adsorptive removal of pharmaceuticals from water by commercial and waste-based carbons. J. Environ. Manag. 152, 83–90. https://doi.org/10.1016/j.jenvman.2015.01.019.

Castaño-Ortiz, J.M., Gil-Solsona, R., Ospina-Álvarez, N., Alcaraz-Hernández, J.D., Farré, M., León, V.M., Barceló, D., Santos, L.H.M.L.M., Rodríguez-Mozaz, S., 2024. Fate of pharmaceuticals in the Ebro River Delta region: the combined evaluation of water, sediment, plastic litter, and biomonitoring. Sci. Total Environ. 906, 167467 https://doi.org/10.1016/j.scitotenv.2023.167467.

Cazetta, A.L., Zhang, T., Silva, T.L., Almeida, V.C., Asefa, T., 2018. Bone char-derived metal-free N- and S-co-doped nanoporous carbon and its efficient electrocatalytic activity for hydrazine oxidation. Appl. Catal., B 225, 30–39. https://doi.org/10.1016/j.apcatb.2017.11.050.

Cha, J.S., Park, S.H., Jung, S.-C., Ryu, C., Jeon, J.-K., Shin, M.-C., Park, Y.-K., 2016. Production and utilization of biochar: a review. J. Ind. Eng. Chem. 40, 1–15. https://doi.org/10.1016/j.jiec.2016.06.002.

Ching, Y., Redzwan, G., 2017. Biological treatment of fish processing saline wastewater for reuse as liquid fertilizer. Sustainability 9, 1062. https://doi.org/10.3390/su9071062.

Côrtes, L.N., Druzian, S.P., Streit, A.F.M., Godinho, M., Perondi, D., Collazzo, G.C., Oliveira, M.L.S., Cadaval, T.R.S., Dotto, G.L., 2019. Biochars from animal wastes as alternative materials to treat colored effluents containing basic red 9. J. Environ. Chem. Eng. 7, 103446 https://doi.org/10.1016/j.jece.2019.103446.

Cruz, M.A.P., Guimarães, L.C.M., da Costa Júnior, E.F., Rocha, S.D.F., Mesquita, P. da L., 2020. Adsorption of crystal violet from aqueous solution in continuous flow system using bone char. Chem. Eng. Commun. 207, 372–381. https://doi.org/10.1080/00986445.2019.1596899.

Egli, M., Rapp-Wright, H., Oloyede, O., Francis, W., Preston-Allen, R., Friedman, S., Woodward, G., Piel, F.B., Barron, L.P., 2023. A One-Health environmental risk assessment of contaminants of emerging concern in London's waterways throughout the SARS-CoV-2 pandemic. Environ. Int. 180, 108210 https://doi.org/10.1016/j.envint.2023.108210.

Ghanizadeh, Gh, Asgari, G., 2011. Adsorption kinetics and isotherm of methylene blue and its removal from aqueous solution using bone charcoal. React. Kinet. Mech. Catal. 102, 127–142. https://doi.org/10.1007/s11144-010-0247-2.

Ghazouani, S., Boujelbane, F., Ennigrou, D.J., Van der Bruggen, B., Mzoughi, N., 2022. Removal of tramadol hydrochloride, an emerging pollutant, from aqueous solution using gamma irradiation combined by nanofiltration. Process Saf. Environ. Protect. 159, 442–451. https://doi.org/10.1016/j.psep.2022.01.005.

Goh, J.Y., Goh, K.S., Yip, Y.M., Ng, C.K., 2022. High salinity enhances the adsorption of 17α-ethinyl estradiol by polyethersulfone membrane: isotherm modelling and molecular simulation. Int. J. Environ. Sci. Technol. 19, 5195–5204. https://doi.org/10.1007/s13762-021-03468-y.

Golovko, O., Örn, S., Sörengård, M., Frieberg, K., Nassazzi, W., Lai, F.Y., Ahrens, L., 2021. Occurrence and removal of chemicals of emerging concern in wastewater treatment plants and their impact on receiving water systems. Sci. Total Environ. 754, 142122 https://doi.org/10.1016/j.scitotenv.2020.142122.

Gomez Cortes, L., Marinov, D., Sanseverino, I., Navarro Cuenca, A., Niegowska, M., Porcel Rodriguez, E., Lettieri, T., 2020. Selection of Substances for the 3rd Watch List under the Water Framework Directive. Publications Office. https://doi.org/10.2760/194067.

Grabicová, K., Grabic, R., Fedorova, G., Vojs Staňová, A., Bláha, M., Randák, T., Brooks, B.W., Žlábek, V., 2020. Water reuse and aquaculture: pharmaceutical bioaccumulation by fish during tertiary treatment in a wastewater stabilization pond. Environ. Pollut. 267, 115593 https://doi.org/10.1016/j.envpol.2020.115593.

Guo, Q., Tang, H., Jiang, L., Chen, M., Zhu, N., Wu, P., 2022. Sorption of $Cd^{2+}$ on bone chars with or without hydrogen peroxide treatment under various pyrolysis temperatures: comparison of mechanisms and performance. Processes 10, 618. https://doi.org/10.3390/pr10040618.

Hajji Nabih, M., El Hajam, M., Boulika, H., Chiki, Z., Ben Tahar, S., Idrissi Kandri, N., Zerouale, A., 2023. Preparation and characterization of activated carbons from cardoon "*Cynara Cardunculus*" waste: application to the adsorption of synthetic organic dyes. Mater. Today Proc. 72, 3369–3379. https://doi.org/10.1016/j.matpr.2022.07.414.

Hashemi, S., Rezaee, A., Nikodel, M., Ganjidost, H., Mousavi, S.M., 2013. Equilibrium and kinetic studies of the adsorption of sodium dodecyl sulfate from aqueous solution using bone char. React. Kinet. Mech. Catal. 109, 433–446. https://doi.org/10.1007/s11144-013-0559-0.

Hernández-Tenorio, R., González-Juárez, E., Guzmán-Mar, J.L., Hinojosa-Reyes, L., Hernández-Ramírez, A., 2022. Review of occurrence of pharmaceuticals worldwide for estimating concentration ranges in aquatic environments at the end of the last decade. J Hazard Mat Adv 8, 100172. https://doi.org/10.1016/j.hazadv.2022.100172.

Hu, X., Gholizadeh, M., 2019. Biomass pyrolysis: a review of the process development and challenges from initial researches up to the commercialisation stage. J. Energy Chem. 39, 109–143. https://doi.org/10.1016/j.jechem.2019.01.024.

James, C.A., Sofield, R., Faber, M., Wark, D., Simmons, A., Harding, L., O'Neill, S., 2023. The screening and prioritization of contaminants of emerging concern in the marine environment based on multiple biological response measures. Sci. Total Environ. 886, 163712 https://doi.org/10.1016/j.scitotenv.2023.163712.

Jia, P., Tan, H., Liu, K., Gao, W., 2018. Synthesis and photocatalytic performance of ZnO/bone char composite. Materials 11, 1981. https://doi.org/10.3390/ma11101981.
Kodešová, R., Švecová, H., Klement, A., Fér, M., Nikodem, A., Fedorova, G., Rieznyk, O., Kočárek, M., Sadchenko, A., Chroňáková, A., Grabic, R., 2024. Contamination of water, soil, and plants by micropollutants from reclaimed wastewater and sludge from a wastewater treatment plant. Sci. Total Environ. 907, 167965 https://doi.org/10.1016/j.scitotenv.2023.167965.
Lamichhane, S., Bal Krishna, K.C., Sarukkalige, R., 2016. Polycyclic aromatic hydrocarbons (PAHs) removal by sorption: a review. Chemosphere 148, 336–353. https://doi.org/10.1016/j.chemosphere.2016.01.036.
Li, Y., Wang, Y., Gao, Y., Zhao, H., Zhou, W., 2018. Seawater toilet flushing sewage treatment and nutrients recovery by marine bacterial-algal mutualistic system. Chemosphere 195, 70–79. https://doi.org/10.1016/j.chemosphere.2017.12.076.
Lightfoot, E.N., 1998. Fundamentals of ceramic powder processing and synthesis. Chem. Eng. Sci. 53, 187.
Lima, F. de A., da Silva, I.P., Vieira, P.V. de O., Rocha, S.D.F., Mesquita, P. da L., 2024. Steam pretreatment of bone char for adsorption of refractory organics from electrodialysis concentrate produced by petroleum refinery. Clean Technol. Environ. Policy 26, 1281–1299. https://doi.org/10.1007/s10098-023-02687-w.
Maged, A., Dissanayake, P.D., Yang, X., Pathirannahalage, C., Bhatnagar, A., Ok, Y.S., 2021. New mechanistic insight into rapid adsorption of pharmaceuticals from water utilizing activated biochar. Environ. Res. 202, 111693 https://doi.org/10.1016/j.envres.2021.111693.
Medellín-Castillo, N.A., González Fernández, L.A., Thiodjio-Sendja, B., Aguilera-Flores, M.M., Leyva-Ramos, R., Reyes-López, S.Y., de León-Martínez, L.D., Dias, J.M., 2023. Bone char for water treatment and environmental applications: a review. J. Anal. Appl. Pyrolysis 175, 106161. https://doi.org/10.1016/j.jaap.2023.106161.
Medellín-Castillo, N.A., Leyva-Ramos, R., Padilla-Ortega, E., Perez, R.O., Flores-Cano, J.V., Berber-Mendoza, M.S., 2014. Adsorption capacity of bone char for removing fluoride from water solution. Role of hydroxyapatite content, adsorption mechanism and competing anions. J. Ind. Eng. Chem. 20, 4014–4021. https://doi.org/10.1016/j.jiec.2013.12.105.
Montes, R., Méndez, S., Cobas, J., Carro, N., Neuparth, T., Alves, N., Santos, M.M., Quintana, J.B., Rodil, R., 2023. Occurrence of persistent and mobile chemicals and other contaminants of emerging concern in Spanish and Portuguese wastewater treatment plants, transnational river basins and coastal water. Sci. Total Environ. 885, 163737 https://doi.org/10.1016/j.scitotenv.2023.163737.
Muretta, J.E., Prieto-Centurion, D., LaDouceur, R., Kirtley, J.D., 2022. Unique Chemistry and structure of pyrolyzed bovine bone for enhanced aqueous metals adsorption. Waste Biomass Valorization 14, 703–722. https://doi.org/10.1007/s12649-022-01895-7.
Panagopoulos, A., 2020. A comparative study on minimum and actual energy consumption for the treatment of desalination brine. Energy 212, 118733. https://doi.org/10.1016/j.energy.2020.118733.
Park, J.-H., Cho, J.-S., Ok, Y.S., Kim, S.-H., Kang, S.-W., Choi, I.-W., Heo, J.-S., DeLaune, R.D., Seo, D.-C., 2015. Competitive adsorption and selectivity sequence of heavy metals by chicken bone-derived biochar: batch and column experiment. J. Environ. Sci. Health, Part A 50, 1194–1204. https://doi.org/10.1080/10934529.2015.1047680.
Park, N., Choi, Y., Kim, D., Kim, K., Jeon, J., 2018. Prioritization of highly exposable pharmaceuticals via a suspect/non-target screening approach: a case study for Yeongsan River, Korea. Sci. Total Environ. 639, 570–579. https://doi.org/10.1016/j.scitotenv.2018.05.081.
Piccirillo, C., 2023. Preparation, characterisation and applications of bone char, a food waste-derived sustainable material: a review. J. Environ. Manag. 339, 117896 https://doi.org/10.1016/j.jenvman.2023.117896.
Piccirillo, C., Moreira, I.S., Novais, R.M., Fernandes, A.J.S., Pullar, R.C., Castro, P.M.L., 2017. Biphasic apatite-carbon materials derived from pyrolysed fish bones for effective adsorption of persistent pollutants and heavy metals. J. Environ. Chem. Eng. 5, 4884–4894. https://doi.org/10.1016/j.jece.2017.09.010.
Piccirillo, C., Pullar, R.C., Costa, E., Santos-Silva, A., Pintado, M.M.E., Castro, P.M.L., 2015. Hydroxyapatite-based materials of marine origin: a bioactivity and sintering study. Mater. Sci. Eng. C 51, 309–315. https://doi.org/10.1016/j.msec.2015.03.020.
Puga, A., Moreira, M.M., Pazos, M., Figueiredo, S.A., Sanromán, M.Á., Delerue-Matos, C., Rosales, E., 2022. Continuous adsorption studies of pharmaceuticals in multicomponent mixtures by agroforestry biochar. J. Environ. Chem. Eng. 10, 106977 https://doi.org/10.1016/j.jece.2021.106977.
Reynel-Avila, H.E., Mendoza-Castillo, D.I., Bonilla-Petriciolet, A., Silvestre-Albero, J., 2015. Assessment of naproxen adsorption on bone char in aqueous solutions using batch and fixed-bed processes. J. Mol. Liq. 209, 187–195. https://doi.org/10.1016/j.molliq.2015.05.013.
Ribeiro, A.R., Castro, P.M.L., Tiritan, M.E., 2012. Chiral pharmaceuticals in the environment. Environ. Chem. Lett. 10, 239–253. https://doi.org/10.1007/s10311-011-0352-0.
Ribeiro, A.R., Santos, L.H.M.L.M., Maia, A.S., Delerue-Matos, C., Castro, P.M.L., Tiritan, M.E., 2014. Enantiomeric fraction evaluation of pharmaceuticals in environmental matrices by liquid chromatography-tandem mass spectrometry. J. Chromatogr. A 1363, 226–235. https://doi.org/10.1016/j.chroma.2014.06.099.
Ribeiro, O., Félix, L., Ribeiro, C., Castro, B., Tiritan, M.E., Monteiro, S.M., Carrola, J.S., 2022. Enantioselective ecotoxicity of venlafaxine in aquatic organisms: Daphnia and zebrafish. Environ. Toxicol. Chem. 41, 1851–1864. https://doi.org/10.1002/etc.5338.
Rúa-Gómez, P.C., Guedez, A.A., Ania, C.O., Püttmann, W., 2012. Upgrading of wastewater treatment plants through the use of unconventional treatment technologies: removal of lidocaine, tramadol, venlafaxine and their metabolites. Water 4, 650–669. https://doi.org/10.3390/w4030650.
Rúa-Gómez, P.C., Püttmann, W., 2012. Occurrence and removal of lidocaine, tramadol, venlafaxine, and their metabolites in German wastewater treatment plants. Environ. Sci. Pollut. Res. 19, 689–699. https://doi.org/10.1007/s11356-011-0614-1.
Scalera, F., Gervaso, F., Sanosh, K.P., Sannino, A., Licciulli, A., 2013. Influence of the calcination temperature on morphological and mechanical properties of highly porous hydroxyapatite scaffolds. Ceram. Int. 39, 4839–4846. https://doi.org/10.1016/j.ceramint.2012.11.076.
Sehonova, P., Hodkovicova, N., Urbanova, M., Örn, S., Blahova, J., Svobodova, Z., Faldyna, M., Chloupek, P., Briedikova, K., Carlsson, G., 2019. Effects of antidepressants with different modes of action on early life stages of fish and amphibians. Environ. Pollut. 254, 112999 https://doi.org/10.1016/j.envpol.2019.112999.
Silva, A., Martinho, S., Stawiński, W., Węgrzyn, A., Figueiredo, S., Santos, L.H.M.L.M., Freitas, O., 2018. Application of vermiculite-derived sustainable adsorbents for removal of venlafaxine. Environ. Sci. Pollut. Res. 25, 17066–17076. https://doi.org/10.1007/s11356-018-1869-6.
Silva, A., Stawiński, W., Romacho, J., Santos, L.H.M.L.M., Figueiredo, S.A., Freitas, O.M., Delerue-Matos, C., 2019. Adsorption of fluoxetine and venlafaxine onto the marine seaweed *Bifurcaria bifurcata*. Environ. Eng. Sci. 36, 573–582. https://doi.org/10.1089/ees.2018.0332.
Silva, C., Ribeiro, C., Maia, A., Gonçalves, V., Tiritan, M., Afonso, C., 2017. Enantiomeric separation of tramadol and its metabolites: method validation and application to environmental samples. Symmetry 9, 170. https://doi.org/10.3390/sym9090170.
Singh, S., Lundborg, C.S., Diwan, V., 2022. Factors influencing the adsorption of antibiotics onto activated carbon in aqueous media. Water Sci. Technol. 86, 2260–2269. https://doi.org/10.2166/wst.2022.334.
Sotelo, J.L., Rodríguez, A., Álvarez, S., García, J., 2012. Removal of caffeine and diclofenac on activated carbon in fixed bed column. Chem. Eng. Res. Des. 90, 967–974. https://doi.org/10.1016/j.cherd.2011.10.012.
Spinelli, F., Dichiarante, E., Curzi, M., Giaffreda, S.L., Chierotti, M.R., Gobetto, R., Rossi, F., Chelazzi, L., Braga, D., Grepioni, F., 2017. Molecular salts of the antidepressant venlafaxine: an effective route to solubility properties modifications. Cryst. Growth Des. 17, 4270–4279. https://doi.org/10.1021/acs.cgd.7b00606.
Sudha, B.S., Sridhar, B.K., Srinatha, A., 2010. Modulation of tramadol release from a hydrophobic matrix: implications of formulations and processing variables. AAPS PharmSciTech 11, 433–440. https://doi.org/10.1208/s12249-010-9400-5.
The Chemistry of processes in the Hydrosphere. In: Environmental Chemistry, 2007. Springer, New York, pp. 96–136. https://doi.org/10.1007/978-0-387-31435-8_6.
Tomczyk, A., Sokołowska, Z., Boguta, P., 2020. Biochar physicochemical properties: pyrolysis temperature and feedstock kind effects. Rev. Environ. Sci. Biotechnol. 19, 191–215. https://doi.org/10.1007/s11157-020-09523-3.
Tsai, C.-Y., Lin, P.-Y., Hsieh, S.-L., Kirankumar, R., Patel, A.K., Singhania, R.-R., Dong, C.-D., Chen, C.-W., Hsieh, S., 2022. Engineered mesoporous biochar derived from rice husk for efficient removal of malachite green from wastewaters. Bioresour. Technol. 347, 126749 https://doi.org/10.1016/j.biortech.2022.126749.
Valverde, S.A., Azevedo, J.C.V., França, A.B., Santos, I.J.B., Naves, F.L., Mesquita, P.L., 2023. Removal of boron from water by batch adsorption onto bovine bone char: optimization, kinetics and equilibrium. Int. J. Environ. Sci. Technol. 20, 9423–9440. https://doi.org/10.1007/s13762-022-04643-5.

Vaudreuil, M.-A., Munoz, G., Vo Duy, S., Sauvé, S., 2024. Tracking down pharmaceutical pollution in surface waters of the St. Lawrence River and its major tributaries. Sci. Total Environ. 912, 168680 https://doi.org/10.1016/j.scitotenv.2023.168680.

Wang, M., Liu, Y., Yao, Y., Han, L., Liu, X., 2020. Comparative evaluation of bone chars derived from bovine parts: physicochemical properties and copper sorption behavior. Sci. Total Environ. 700, 134470 https://doi.org/10.1016/j.scitotenv.2019.134470.

Wu, X., Liu, P., Huang, H., Gao, S., 2020. Adsorption of triclosan onto different aged polypropylene microplastics: critical effect of cations. Sci. Total Environ. 717, 137033 https://doi.org/10.1016/j.scitotenv.2020.137033.

Wurzer, C., Oesterle, P., Jansson, S., Mašek, O., 2023. Hydrothermal recycling of carbon absorbents loaded with emerging wastewater contaminants. Environ. Pollut. 316, 120532 https://doi.org/10.1016/j.envpol.2022.120532.

Xiang, Y., Xu, Z., Wei, Y., Zhou, Y., Yang, X., Yang, Y., Yang, J., Zhang, J., Luo, L., Zhou, Z., 2019. Carbon-based materials as adsorbent for antibiotics removal: mechanisms and influencing factors. J. Environ. Manag. 237, 128–138. https://doi.org/10.1016/j.jenvman.2019.02.068.

Yadav, A., Bagotia, N., Sharma, A.K., Kumar, S., 2021. Simultaneous adsorptive removal of conventional and emerging contaminants in multi-component systems for wastewater remediation: a critical review. Sci. Total Environ. 799, 149500 https://doi.org/10.1016/j.scitotenv.2021.149500.

Zhang, D., Yin, J., Zhao, J., Zhu, H., Wang, C., 2015. Adsorption and removal of tetracycline from water by petroleum coke-derived highly porous activated carbon. J. Environ. Chem. Eng. 3, 1504–1512. https://doi.org/10.1016/j.jece.2015.05.014.